Supporting Information

ZnO-Based Nanoplatforms for Labeling and Treatment of Mouse Tumors without Detectable Toxic Side Effects

Dai-Xin Ye, Ying-Ying Ma, Wei Zhao, Hong-Mei Cao, Ji-Lie Kong,* Huan-Ming Xiong* and Helmuth Möhwald

E-mail: jlkong@fudan.edu.cn or hmxiong@fudan.edu.cn

Figures and Captions

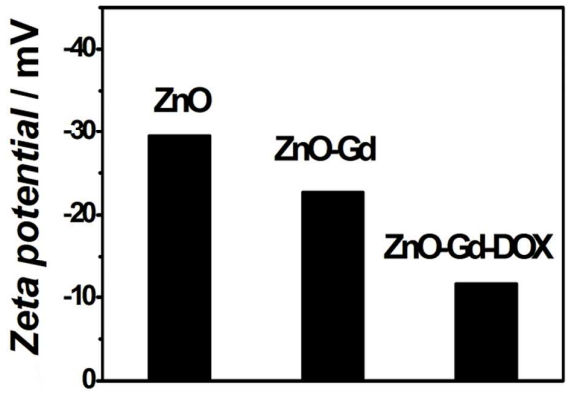

Figure S1. Zeta potentials of ZnO, ZnO-Gd and ZnO-Gd-DOX NPs in water.

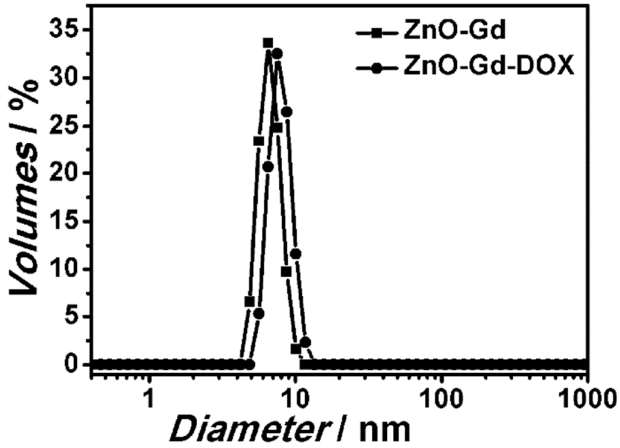

Figure S2. Dynamic light scattering (DLS) data of ZnO-Gd and ZnO-Gd-DOX NPs in water.

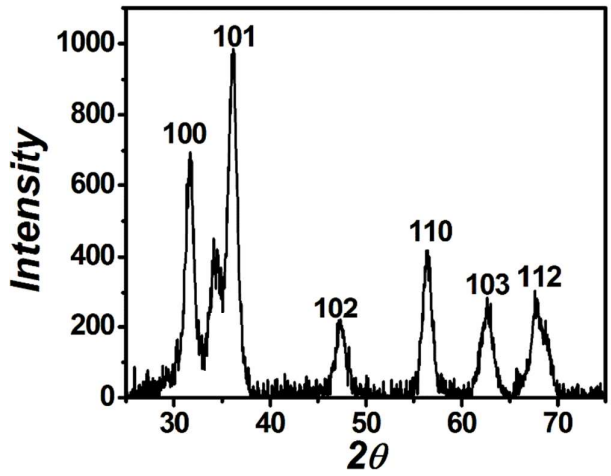

Figure S3. X-ray diffraction patterns of ZnO-Gd NPs.

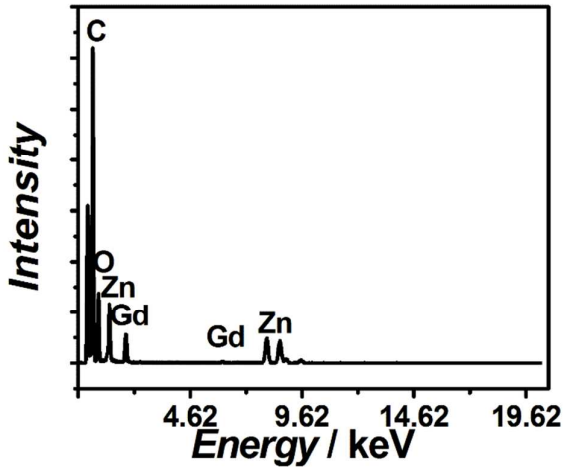

Figure S4. Energy Dispersive X-ray (EDX) spectrum of ZnO-Gd NPs.

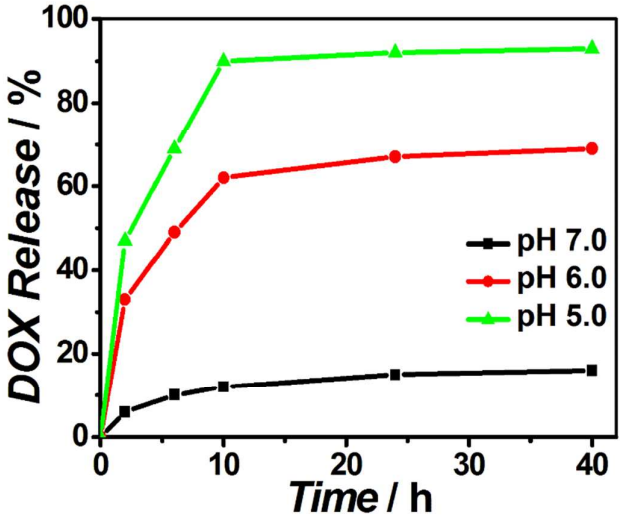

Figure S5. DOX release profile of ZnO-Gd-DOX NPs at different pH values.

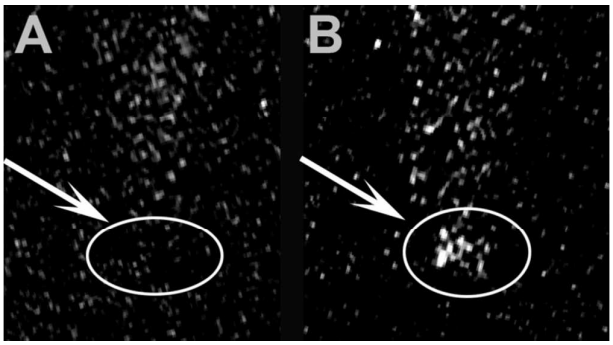

Figure S6. T_1-weighted images of (A) blank BxPC-3 cells and (B) BxPC-3 cells incubated with ZnO-Gd-DOX NPs (corresponding to 0.06 mM of Gd^{3+} ions) for 1.5 h. The marked area in (B) is evidently brighter than that in (A), which shows the precipitation of cells in a centrifuge tube after centrifugation, indicating that ZnO-Gd-DOX NPs can serve as effective MRI contrast agent.

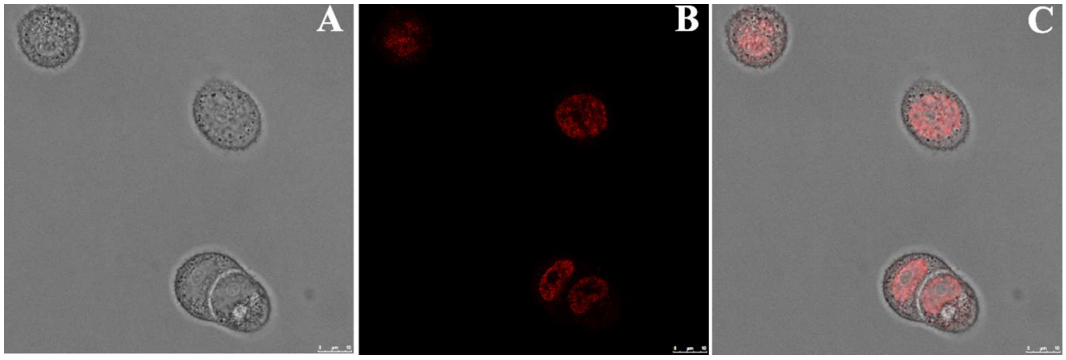

Figure S7. After incubation with ZnO-Gd-DOX NPs for 1.5 h at 37 ^{o}C, the CLSM images of BxPC-3 cells in (A) bright field, (B) fluorescence field under 488 nm of excitation, and (C) the overlay of (A) and (B). Each scale bar represents 10 μm. It is apparent, that the ZnO-Gd-DOX NPs have entered the cells and decomposed to release DOX, and the DOX has penetrated into the nuclei. However, the nucleoli inside the nuclei are not stained by DOX.

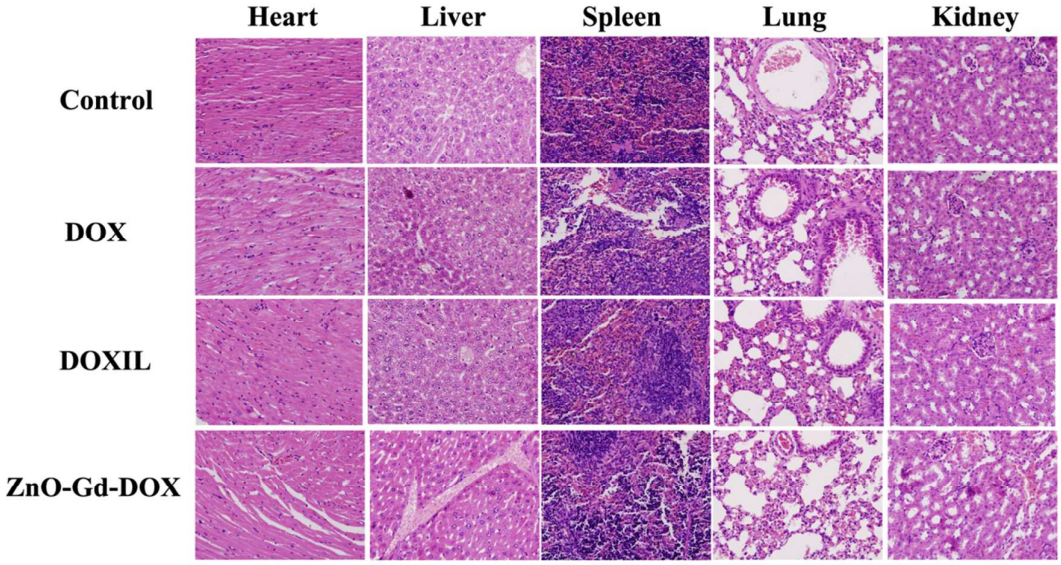

Figure S8. H&E stained images of major organs collected from the tumor-bearing mice treated with different agents (DOX, DOXIL and ZnO-Gd-DOX are at the DOX dosage of 2 mg/kg; Control is injected with 200 μL of saline).

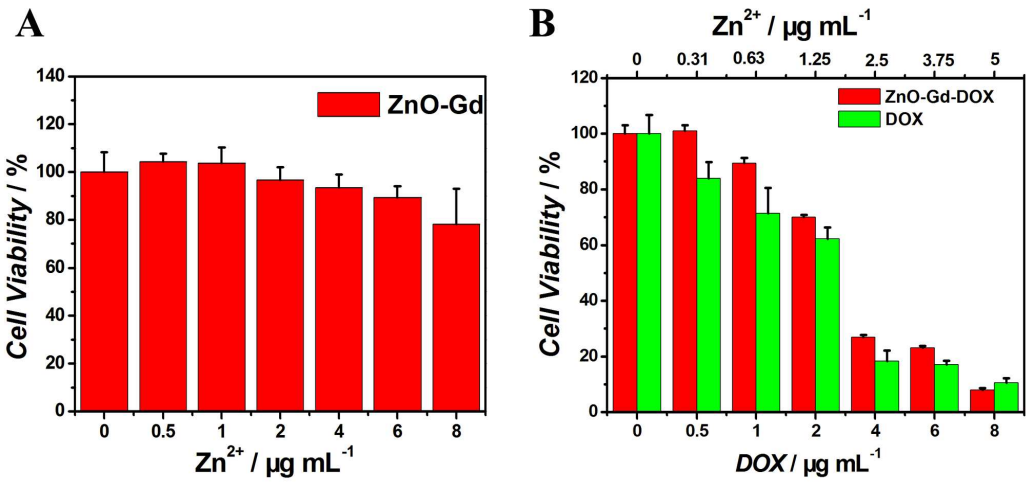

Figure S9. Viability of the BxPC-3 cells after 24 h incubation with (A) ZnO-Gd NPs, (B) ZnO-Gd-DOX NPs and DOX, respectively.

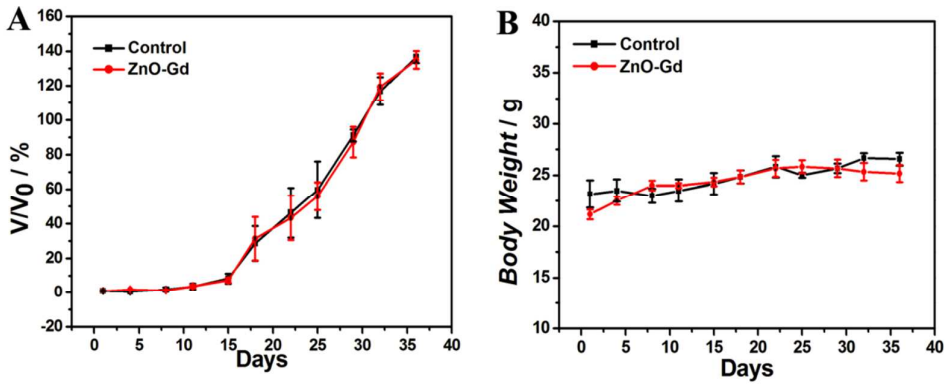

Figure S10. (A) Tumor growth curves and (B) Body weight evolutions of the BxPC-3 bearing mice with ZnO-Gd solution and saline (control) injected, respectively. The dosage of ZnO-Gd is 1.25 mg/kg of Zn^{2+} ions in each injection.

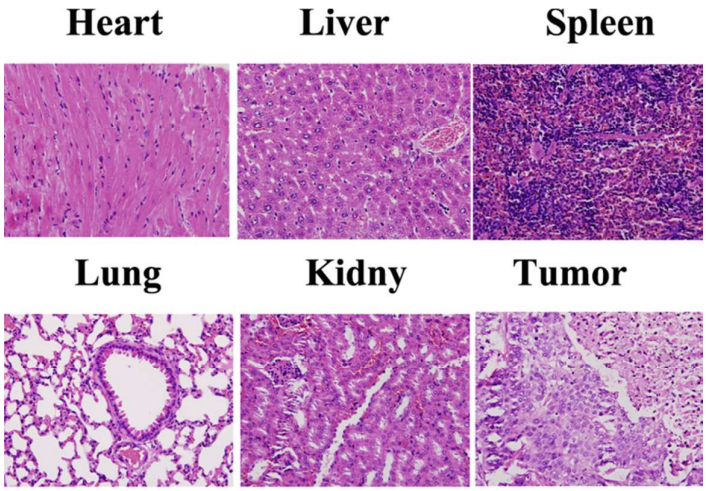

Figure S11. H&E stained images of the major organs collected from the tumor-bearing mice after 36 days' treatment by ZnO-Gd solution with 1.25 mg/kg of Zn^{2+} ions in each injection.

Table S1. Comparison of relaxivities of T_1 contrast agents based on Gd^{3+}-ligand complexes.

Composition	**$r_1(mM^{-1}s^{-1})$**	**$r_2(mM^{-1}s^{-1})$**	**r_2/r_1**	**Field(T)**
Gd-AuNC[1]	41.5	49.6	1.2	0.55
GO−DTPA−Gd[2]	10.8			11.7
h-P(CPTM-co-DOTA-(Gd))-b-P(OEGMA-co-GPMA) [3]	3.12			1.5
Added 2 μM DTT in the above solution [3]	4.04			1.5
Added 10 mM DTT in the above solution [3]	29.92			1.5
Added 20 mM DTT in the above solution [3]	35.97			1.5
HSP-BP-DTPA-Gd [4]	25			0.73
gold nanorods-GdDTPAA[5]	21.3			9.4
PbdEO/PEOCL: Gd-DTPA-G3[6]	7.5			1.41
Gd-TREN-bis-HOPO-TAM-ethylamine-EA[7]	38			1.41
Gd-TREN-bis-HOPO-TAM-ethylamine-PLL[7]	21			1.41
DNA-Gd^{III}@AuNP-13 nm[8]	16.9			1.41
DNA-Gd^{III}@AuNP-30 nm[8]	20			1.41
DNA-Gd^{III}[8]	8.7			1.41
MS2-HOPO-Lin[9]	29.7			1.41
MS2-HOPO-SS[9]	38.2			1.41
MS2-HOPO-RR[9]	25.4			1.41
Gd-DTPA (this work)	3.7	4.2	1.1	0.55
$GdCl_3$ (this work)	8.12	9.28	1.14	0.55

Table S2. Comparison of relaxivities of T_1 contrast agents based on inorganic nanoparticles.

Composition	$r_1(mM^{-1}s^{-1})$	$r_2(mM^{-1}s^{-1})$	r_2/r_1	Field (T)
GHC-1[10]	34.8	40.6	1.17	0.55
a-$NaGdF_4$:Yb^{3+}:Er^{3+}/$NaGdF_4$[11]	1.4			1.5
PGP/dextran-K01[12]	13.9	15.0	1.1	0.47
$Gd_{0.6}Eu_{0.4}VO_4/SiO_2$[13]	2.52	3.03	1.2	
$Gd_{0.6}Eu_{0.4}VO_4$[13]	2.97	3.47	1.17	
$GdVO_4$[13]	0.95	1.31	1.08	
$GdVO_4^{cit13}$	4.6	5.52	1.2	
$Gd_{0.6}Eu_{0.4}VO_4^{cit13}$	8.18	9.38	1.15	
GadoSiPEG[14]	8.8	11.4	1.3	7
Gd_2O_3[15]	9.9	10.5	1.1	1.5
HMnO@$mSiO_2$[16]	1.72	11.3	6.6	1.5
HMONs[17]	1.42	7.74	5.5	3.0
Core@$NaGdF_4$[18]	6.18			3.0
$KGdF_4$[19]	5.86			9.4
UCNPs[20]	1.40			1.5
UCNPs@$mSiO_2$-ZnO[21]	4.78			1.5
Gd-doped ZnO QDs[22]	16			1.5
ZnO-Gd (this work)	49.5	63	1.27	0.55
ZnO-Gd-DOX (this work)	52.5	66.5	1.26	0.55

References

1 Liang G. H.; Ye D. X.; Zhang X. X.; Dong F.; Chen H.; Zhang S.; Li J. Q.; Shen X. R.; Kong J. L. One-Pot Synthesis of Gd^{3+}-Functionalized Gold Nanoclusters for Dual Model (Fluorescence/Magnetic Resonance) Imaging. *J. Mater. Chem. B* **2013**, *1*, 3545.

2 Zhang M. X.; Cao Y. H.; Chong Y.; Ma Y. F.; Zhang H. L.; Deng Z. W.; Hu C. H.; Zhang Z. J. Graphene Oxide Based Theranostic Platform for T_1-Weighted Magnetic Resonance Imaging and Drug Delivery. *ACS Appl. Mater. Inter.* **2013**, *5*, 13325.

3 Liepold L. O.; Abedin M. J.; Buckhouse E. D.; Frank J. A.; Young M. J.; Douglas T. Supramolecular Protein Cage Composite MR Contrast Agents with Extremely Efficient Relaxivity Properties. *Nano Lett.* **2009**, *9*, 4520.

4 Kim H. K.; Park J. A.; Kim K. M.; Md N. S.; Kang D. S.; Lee J.; Chang Y.; Kim T. J. Gd-Complexes of Macrocyclic DTPA Conjugates of 1,10 -Bis(amino)Ferrocenes as High Relaxivity MRI Blood-Pool Contrast Agents (BPCAs). *Chem. Comm.* **2010**, *46*, 8442.

5 Sun H. M.; Yuan Q. H.; Zhang B. H.; Ai K. L.; Zhang P. G.; Lu L. H.; Gd^{III} Functionalized Gold Nanorods for Multimodal Imaging Applications. *Nanoscale* **2011**, *3*, 1990.

6 Cheng Z. L.; Thorek D.; Tsourkas A. Porous Polymersomes with Encapsulated Gd-Labeled Dendrimers as Highly Efficient MRI Contrast Agents. *Adv. Funct. Mater.* **2009**, *19*, 3753.

7 Floyd W. C.; Klemm P. J.; Smiles D. E.; Kohlgruber A. C.; Pierre V. C.; Mynar J. L.; Frechet J.; Raymond K. N. Conjugation Effects of Various Linkers on Gd(III) MRI Contrast Agents with Dendrimers: Optimizing the Hydroxypyridinonate (HOPO) Ligands with Nontoxic, Degradable Esteramide (EA) Dendrimers for High Relaxivity. *J. Am. Chem. Soc.***2011**, *133*, 2390.

8 Song Y.; Xu X. Y.; MacRenaris K. W.; Zhang X. Q.; Mirkin C. A.; Meade T. J. Multimodal Gadolinium-Enriched DNA–Gold Nanoparticle Conjugates for Cellular Imaging. *Angew. Chem. Int. Ed.* **2009**, *48*, 9143.

9 Garimella P. D.; Datta A.; Romanini D. W.; Raymond K. N.; Francis M. B. Multivalent, High-Relaxivity MRI Contrast Agents Using Rigid Cysteine-Reactive Gadolinium Complexes. *J. Am. Chem. Soc.* **2011**, *133*, 14704.

10 Liang G. H.; Cao L. L.; Chen H.; Zhang Z. Y.; Zhang S.; Yu S. N.; Shen X. R.; Kong J. L. Ultrasmall Gadolinium Hydrated Carbonate Nanoparticle: An Advanced T_1 MRI Contrast Agent with Large Longitudinal Relaxivity. *J. Mater. Chem. B* **2013**, *1*, 629.

11 Park Y. I.; Kim J. H.; Lee K. T.; Jeon K. S.; Na H. Bin; Yu J. H.; Kim H. M.; Lee N.; Choi S. H., Baik S. I.; Kim H.; Park S. P.; Park B. J.; Kim Y. W.; Lee S. H.; Yoon S. Y.; Song I. C.; Moon W. K.; Suh Y. D.; Hyeon T.; Nonblinking and Nonbleaching Upconverting Nanoparticles as an Optical Imaging Nanoprobe and T_1 Magnetic Resonance Imaging Contrast Agent. *Adv. Mater.* **2009**, *21*, 4467.

12 Hifumi H.; Yamaoka S.; Tanimoto A.; Citterio D.; Suzuki K. Gadolinium-Based Hybrid Nanoparticles as a Positive MR Contrast Agent. *J. Am. Chem. Soc.* **2006**, *128*, 15090.

13 Abdesselem M.; Schoeffel M.; Maurin I.; Ramodiharilafy R.; Autret G.; Clement O.; Tharaux P. L.; Boilot J. P.; Gacoin T.; Bouzigues C.; Alexandrou A. Multifunctional Rare-Earth Vanadate Nanoparticles: Luminescent Labels, Oxidant Sensors, and MRI Contrast Agents. *ACS Nano* **2014**, *8*, 11126.

14 Bridot J. L.; Faure A. C.; Laurent S.; Riviere C.; Billotey C.; Hiba B.; Janier M.; Josserand V.; Coll J. L.; Elst L. Vander; Muller R.; Roux S.; Perriat P.; Tillement O. Hybrid Gadolinium Oxide Nanoparticles: Multimodal Contrast Agents for in Vivo Imaging. *J. Am. Chem. Soc.* **2007**, *129*, 5076.

15 Park J. Y.; Baek M. J.; Choi E. S.; Woo S.; Kim J. H.; Kim T. J.; Jung J. C.; Chae K. S.; Chang Y.; Lee G. H. Paramagnetic Ultrasmall Gadolinium Oxide Nanoparticles as Advanced T_1 MRI Contrast Agent: Account for Large Longitudinal Relaxivity, Optimal Particle Diameter, and *In Vivo* T_1 MR Images. *ACS Nano* **2009**, *3*, 3663.

16 Kim T.; Momin E.; Choi J.; Yuan K.; Zaidi H.; Kim J.; Park M.; Lee N.; McMahon M. T.; Quinones-Hinojosa A.; Bulte J.; Hyeon T.; Gilad A. A. Mesoporous Silica-Coated Hollow Manganese Oxide Nanoparticles as Positive T_1 Contrast Agents for Labeling and MRI Tracking of Adipose Derived Mesenchymal Stem Cells. *J. Am. Chem. Soc.* **2011**, *133*, 2955.

17 Shin J. M.; Anisur R. M.; Ko M. K.; Im G. H.; Lee J. H.; Lee I. S. Hollow Manganese Oxide Nanoparticles as Multifunctional Agents for Magnetic Resonance Imaging and Drug Delivery. *Angew. Chem. Int. Ed.* **2009**, *48*, 321.

18 Chen F.; Bu W. B.; Zhang S. J.; Liu X. H.; Liu J. N.; Xing H. Y.; Xiao Q. F.; Zhou L. P.; Peng W. J.; Wang L. Z.; Shi J. L. Positive and Negative Lattice Shielding Effects Co-existing in Gd (III) Ion Doped Bifunctional Upconversion Nanoprobes. *Adv. Funct. Mater.* **2011**, *21*, 4285.

19 Ju Q.; Tu D. T.; Liu Y. S.; Li R. F.; Zhu H. M.; Chen J. C.; Chen Z.; Huang M. D.; Chen X. Y. Amine-Functionalized Lanthanide-Doped $KGdF_4$ Nanocrystals as Potential Optical/Magnetic Multimodal Bioprobes. *J. Am. Chem. Soc.* **2012**, *134*, 1323.

20 Park Y. I.; Kim J. H.; Lee K. T.; Jeon K. S.; Na H. Bin; Yu J. H.; Kim H. M.; Lee N.; Choi S. H.; Baik S. I.; Kim H.; Park S. P.; Park B. J.; Kim Y. W.; Lee S. H.; Yoon S. Y.; Song I. C.; Moon W. K.; Suh Y. D.; Hyeon T. Nonblinking and Nonbleaching Upconverting Nanoparticles as an Optical Imaging Nanoprobe and T1 Magnetic Resonance Imaging Contrast Agent. *Adv. Mater.* **2009**, *21*, 4467.

21 Wang Y. H.; Song S. Y.; Liu J. H.; Liu D. P.; Zhang H. J. ZnO-Functionalized Upconverting Nanotheranostic Agent: Multi-Modality Imaging-Guided Chemotherapy with On-Demand Drug Release Triggered by pH. *Angew. Chem. Int. Ed.* **2015**, *54*, 536.

22 Liu Y. L.; Ai K. L.; Yuan Q. H.; Lu L. H. Fluorescence-Enhanced Gadolinium-Doped Zinc Oxide Quantum Dots for Magnetic Resonance and Fluorescence Imaging. *Biomaterials* **2011**, *32*, 1185.